Evaluation of vertebral injuries in dogs using computed tomography

Venkatesh V[1, *], Vijayakumar M[2], Kathirvel S[3] and Balasundaram K[4].

[1*,2 and 3] *Department of Veterinary Surgery and Radiology, [4]Department of Veterinary Anatomy, Veterinary College and Research Institute, Namakkal, Tamil Nadu Veterinary and Animal Sciences University-Chennai, Tamil Nadu, India-637002.*

ABSTRACT

Background: *Spinal disorders in dogs are usually associated with some neurologic dysfunctions like paresis or paraplegia and more common in thoracolumbar spinal segment. Survey radiography and myelography are commonly used for the diagnosis of spinal disorders but with poor diagnostic efficiency. Computed tomographic (CT) is an emerging important diagnostic tool, especially in canine orthopaedic cases and provide advantage over radiographs.*

Methods: *The study was carried out in dogs brought to Veterinary Clinical Complex, Veterinary College and Research Institute, Namakkal, Tamil Nadu, India during the period from January to December 2021. Study was carried out for evaluating the radiological and computed tomographical findings in twelve dogs, divided into group I (normal dogs) and group II (with spinal disorders). Neurological examination, survey radiography and computed tomography was performed. Lateral and ventrodorsal radiograph of the spine were taken as localized by neurological evaluation. CT was performed using 16 slice CT unit (Toshiba).*

Result: *Radiography and computed tomography were performed in all dogs of group I and II. Group I dogs, revealed normal spinal anatomical features whereas group II dogs with varies vertebral lesions were diagnosed. Radiograph provided the anatomical land mark for major lesion with only limited, and indirect diagnostic details, whereas CT evaluation revealed more details about the various spinal bony lesions. Thus, it is concluded that computed tomography was non-invasive, highly sensitive 3D imaging technique in diagnosing spinal injuries of dogs than conventional radiography.*

Key words: *Fracture, Computed tomography, Dogs, Radiography*

I. INTRODUCTION

Survey radiography and myelography are the most routinely used method for the diagnosis of spinal diseases in veterinary practice. But the main disadvantage with both the methods are poor diagnostic efficiency in ruling out the degree of acute vertebral injury, compression and to assess the stability of spinal fracture. CT is highly sensitive to the presence of bony lesions and is the modality of choice as a first line approach to the human polytrauma patients (Kinns *et al*. 2006). Multidetector computed tomography has transformed computed tomography technology by providing near-isotropic volumetric representation of the complete body with exquisite anatomical details in brief scan time. Post processing techniques multiplanar reconstruction and volume rendering by three-dimension (3D) images are very helpful for accurate surgical planning (Ricciardi. 2016).

CT images has more advantage over conventional radiographs that, in former the image is depicted without the effects of superimposition and has superior soft tissue differentiation (contrast resolution) as well as the spatial resolution is also far superior. Hence, it also necessitates a step forward to CT application in veterinary medicine to make better diagnosis of spinal injuries. Nowadays, CT is becoming a sensitive, non-invasive diagnostic and evaluating technique in veterinary practice and an efficient tool to image canine spine and its lesions.

II. MATERIALS AND METHODS

2.1 NEUROLOGICAL EXAMINATION

2.1.1 Postural reactions examination: Postural reactions include conscious proprioception, wheelbarrow, hopping, and hemi-walking were examined to distinguish neurological disorders from diseases of other body systems. Abnormalities like absence or reduction in postural reactions were recorded (Palus, 2014).

2.1.2 Spinal reflexes examination: Various spinal reflexes *viz* biceps, triceps, extensor carpi, flexor tendon, withdrawal and crossed extensor of thoracic limbs and the spinal reflexes of pelvic limb such as patellar reflex,

gastrocnemius reflex, cranial tibial reflex, sciatic reflex, withdrawal reflex and crossed extensor reflex were examined and graded as 0- Absent, 1- Decreased, 2- Normal and 3- Increased. Other spinal reflexes like anal reflex, panniculus reflex, neck pain and back pain were also recorded as present or absent as described by Taylor (2009).

2.1.3 Localization of spinal lesion: Localization of lesion in the spinal cord segment was performed based on involvement of UMN and LMN as described by Denny and Butterworth (2000)

2.1.4 Grading of spinal cord lesion: Based on neurological examination severity of the spinal cord injury were graded from 1 to 7 (Denny and Butterworth, 2000).

Grade 1: Pain only

Grade 2: Ambulatory paraparesis / quadriparesis

Grade 3: Non-ambulatory paraparesis / quadriparesis

Grade 4: Paraplegia/quadriplegia

Grade 5: Paraplegia/quadriplegia + urinary retention with overflow (URO)

Grade 6: Paraplegia/quadriplegia + URO + loss of conscious pain sensation (CPS)

Grade 7: Ascending/descending myelomalacia

For the diagnostic procedure dogs were sedated with Inj. Dexmedetomidine at a dose rate of 5 µg/kg body weight intravenously and with Inj. Butorphanol at a dose rate of 0.2 mg/kg body weight intravenously.

2.2 CT scanner and Imaging procedure: CT scanning was done by using third generation 16 slice Alexion multi slice computed tomography (MSCT) scanner manufactured by Toshiba company, Japan and CT images obtained using post-processing vitrea software. All procedures are done in a cranial to caudal direction. Transverse slices were obtained from lateral and ventro dorsal scout image of spine from first cervical vertebrae to coccygeal vertebrae (Dabanoglu *et al*. 2004).

2.3 Acquisition parameters: In the present study, tube voltage of 120 kV was maintained constant as it represents the penetration of the X-rays and tube current of 70 mAs was used for CT scan as it represents the radiographic exposure (Ricciardi, 2016).

2.4 Slice thickness: Slice thickness is the single most important setting to select for a CT scan to obtain adequate details and sufficient spatial resolution in all planes *viz* sagittal, coronal and transverse. Slice thickness of 1mm has been set especially for detailed post processing evaluation using Multiplanar Reformation (MPR) studies (Ricciardi, 2016).

2.5 Pitch: Pitch represents the ratio of table speed per gantry rotation around the patient. For this study 0.75 seconds had been chosen (Tins, 2010).

2.6 CT post processing techniques

2.6.1 Algorithm: Bone and soft tissue algorithm were chosen for post processing reconstruction of images from raw data (Ricciardi, 2016).

2.6.2 Multiplanar reformation (MPR): Multiplanar reformation is a two-dimensional technique. The original transverse data is reformatted into additional planes – coronal, sagittal, and transverse. Spinal injuries have evaluated in multiple planes (Bertolini and Prokop, 2011).

2.6.3 Three-dimensional image (3 D image): 3D image is most flexible visualization tool, it benefits when presenting information to clients. Lesions are much easier for layperson to understand when visualized in this method and planning of fracture repair can be improved by 3D visualization of the injury (Schwarz *et al*. 2000).

2.7 Evaluation of the stability of traumatic spinal injuries: Stability of traumatic spinal injuries were assessed according to the three-column spine principle. The vertebral column can be divided into three compartments: dorsal, middle, and ventral. Injuries in more than one of these three compartments was considered as very unstable (Ricciardi, 2016). Fig.1**.**
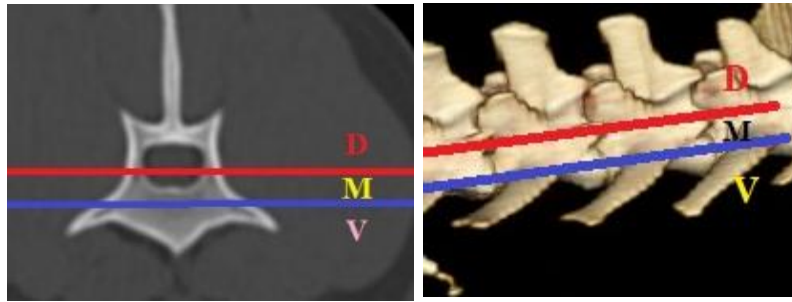
Three column spine principle for assessing stability of traumatic injuries
Figure 1: Evaluation of the stability of traumatic spinal injuries

IV. RESULT AND DISCSSION

4.1 NEUROLOGICAL EXAMINATION

4.1.1 Postural reactions examination: Group I dogs showed no postural abnormalities whereas dogs in group II showed abnormalities like absence or reduced postural reactions in thoracic or pelvic limbs and are presented in table 1.

4.1.2 Spinal reflexes examination: Abnormalities in spinal reflexes like withdrawal, patellar and deep pain reflexes were not observed in group I however it was observed in group II dogs in various states and are presented in table 2.

4.1.3 Localization and grading of spinal cord lesion: All six dogs in group II showed the signs of upper motor neuron (UMN) deficit by having lesion in T_3 to L_3 segments, while locating lesion on the spinal cord segment. The spinal cord lesion is graded as per standard method. The results are presented in table 3.

Radiographic and computed tomographic examination

Transverse CT image of group I dogs disclosed the normal spinal structures with a mean CT density of cortical and cancellous bone were +1202.9 ± 67.8 HU and + 422.6 ± 54.8 HU, respectively in bony vertebrae. The mean CT density of the normal intervertebral disc was +164 ± 44.1 HU at the centre and + 463.4 ± 55.4 HU at the periphery in bony window and intervertebral disc was not visualized in soft tissue window. Mean CT density of the spinal cord in normal dogs was + 32.9 ± 15.9 HU. Thoracic vertebrae were identified by the presence of the ribs bilaterally whereas lumbar vertebrae are clearly evident lateral to the vertebral bodies and is presented in Fig. 2.

Table 1: Postural reactions

Case	Thoracic limb					Pelvic limb				
	CP		WB	H		CP		WB	H	
	Rt	Le		Rt	Le	Rt	Le		Rt	Le
1	N	N	N	N	N	A	A	A	A	A
2	N	N	N	R	R	N	N	N	R	R
3	N	N	N	N	N	A	A	A	A	A
4	N	N	N	N	N	A	A	A	A	A
5	N	N	N	N	N	N	N	N	N	N
6	N	N	N	N	N	R	R	R	A	A

CP: Conscious proprioception   WB: Wheelbarrowing   H: Hopping   Rt: Right   Le: left
N: Normal   A: Absent   R: Reduced

Table 2: Spinal reflexes

Case	Breed	Thoracic limb				Pelvic limb					
		W		DP		W		PAT		DP	
		Rt	Le	Rt	Le	Rt	Le	Rt	Le	Rt	Le
1	Mongrel	2	2	2	2	2	2	3	3	2	2
2	Dobermann	2	2	2	2	1	1	2	2	2	2
3	Mongrel	2	2	2	2	0	0	0	0	0	0
4	Mongrel	2	2	2	2	0	0	1	1	1	1
5	Mongrel	2	2	2	2	2	2	2	2	2	2
6	Dachshund	2	2	2	2	0	0	3	3	2	2

W: Withdrawal	DP: Deep Pain	PAT: Patellar	Rt: Right	Le: left
0: Absent	1: Decreased	2: Normal	3: Increased	

Table 3: Localization of lesion on spinal cord segment and grading

Cases	Thoracic limbs	Pelvic limbs	Localized spinal cord segment	Grade
1	N	UMN	T_3-L_3 segment	5
2	N	UMN	T_3-L_3 segment	1
3	N	UMN	T_3-L_3 segment	5
4	N	UMN	T_3-L_3 segment	6
5	N	UMN	T_3-L_3 segment	1
6	N	UMN	T_3-L_3 segment	2

N- Normal,   UMN- Upper Motor Neuron,   LMN- Lower Motor Neuron.

Case 1: Survey radiograph revealed vertebral body compression at level of T_{13} and L_1. Sagittal plane of CT thoraco-lumbar region revealed simultaneous occurrence of axial compression at L_1 in the caudo-cranial direction and fracture of the left transverse process seen in coronal, axial and 3D volume rendering images respectively were presented in Fig. 3.

Case 2: Periosteal new bone formation of the ventral and lateral margins was observed from T_{13} to L_2 and between L_6-L_7 on plain radiography, whereas CT revealed hypoattenuation of vertebral end plates from T_{13} to L_2. Fig. 4. Transverse CT image was useful in evaluating the migration of osteophytes into the spinal canal and cord compression. Spondylosis was observed in vertebrae other than the primary lesion segment which caused the neurological deficit. In some cases, even though the spondylosis was observed, it was not a sole etiology for neurological signs because invasion of ventral osteophyte into the spinal canal and spinal nerve compression was not possible whereas spondylosis with disc herniation was possible for nerve root compression. These findings were concurred with the observations of Akeda *et al.* (2015).

Case 3: Thoracolumbar spinal radiograph caudal physeal fracture of L_1 vertebrae. CT axial plane revealed fracture fragment displaced in the vertebral canal and compressing the spinal cord. Sagittal plane revealed fracture of L_1 vertebral body with luxation of caudal part to the L_1 vertebrae. As the fracture is involving more than two compartments considered as unstable. Fig. 5.

Case 4: Plane radiograph revealed axial compression fracture of the L_3 vertebra. CT axial plane revealed multiple fragments displaced in the vertebral canal (multifragmentated fracture of L_3 vertebra). Sagittal and axial planes revealed as bursting fracture of L_3 vertebrae due to axial compression force. 3D volume rendering of ventrodorsal view revealed L_3 burst fracture with left transverse process fracture of L_4 vertebra. Fig. 6.

Case 5: Dog showed head tilt towards right side during physical examination and on plain radiography of ventrodorsal view revealed atlas left wing green stick fracture. CT coronal plane and 3D volume rendering revealed fracture of left wing of atlas along with slight luxation of the axis towards left side. Fig. 7.

Case 6: Lateral radiography revealed excessive mineralization of intervertebral disc and narrowing of both intervertebral space and foramen between L_1 to L_2. CT revealed multiple hyperattenuating mass in between the intervertebral body of T_{2-3}, T_{7-8}, T_{10-11} and L_{1-2} on transverse plane, while at the same time transverse section of L_{1-2} revealed the round focus of hyperattenuating material in the floor of the vertebral canal indicative of severe spinal compression with density of $+1086.7 \pm 293.4$ HU (Fig.8). In present study, herniation of mineralized disc material into the vertebral canal was apparent even without the injection of subarachnoid contrast medium. CT density of the spinal cord was $+32.9\pm15.9$ HU whereas the CT density of the herniated disc was $+1086.7\pm293.4$ HU in soft tissue window. Hence, hyper attenuation variation could be helpful in diagnosing disc herniation (Olby *et al.* 2000; Lim *et al.*, 2010).

In the present study, thoracolumbar spine was found to be the common site for fracture in all the cases, which could be attributed due to its location between the rigid thoracic spine and the well-muscled lumbar spine (Ricciardi, 2016; Bagley, 2000). Among the six cases, four were found to be associated with road traffic accident leads to various types fracture like compression, Atlas wing and burst fracture.

Fracture was seen in all three dorsal, middle and ventral compartments in cases no 3 and 4, respectively and stability of the fracture was assessed according to the three-column spine principle. Vertebral column was divided into three compartments: the dorsal compartment includes the spinous process, vertebral laminae, articular processes, vertebral pedicles and dorsal ligamentous complex (supraspinous ligament, interspinous ligament, joint capsule, ligamentum flavum). The middle compartment includes the dorsal longitudinal ligament, dorsal annulus fibrosis and dorsal vertebral body. The ventral compartment includes the remaining vertebral body, lateral and ventral aspects of annulus fibrosus, the nucleous pulposus and the ventral longitudinal ligament. Regardless of the degree of displacement of fracture, damage in two or more components were considered as unstable and suggested for surgical stabilization. This is in accordance with Kinns *et al.* (2006) and Ricciardi (2016).

Thus, it can be concluded that survey radiograph which is the first line of approach for diagnosis of spinal injuries in dogs, provided the anatomical land mark for major lesion with only limited details about the spinal injuries. The two-dimension nature of the radiograph along with superimposition by unrelated structure made it too difficult to visualize minute details of spinal injuries. CT endowed with contrast resolution with tomographic nature of prevented problem of superimposition, normally seen in typical radiograph. Thus, it makes CT, an ideal three-dimensional diagnostic technique for the characterization and localization of traumatic lesions affecting bones together with complex structure such as vertebrae, associated with position of fragments in relation to the spinal canal.

A) 3D image of normal spine; B) Cervical vertebra (C_6); C) Thoracic vertebra; D) Lumbar vertebra; E) Sacrum; F) Image showing normal density of cortical, cancellous bone and spinal cord; G) Image showing normal density of intervertebral disc.
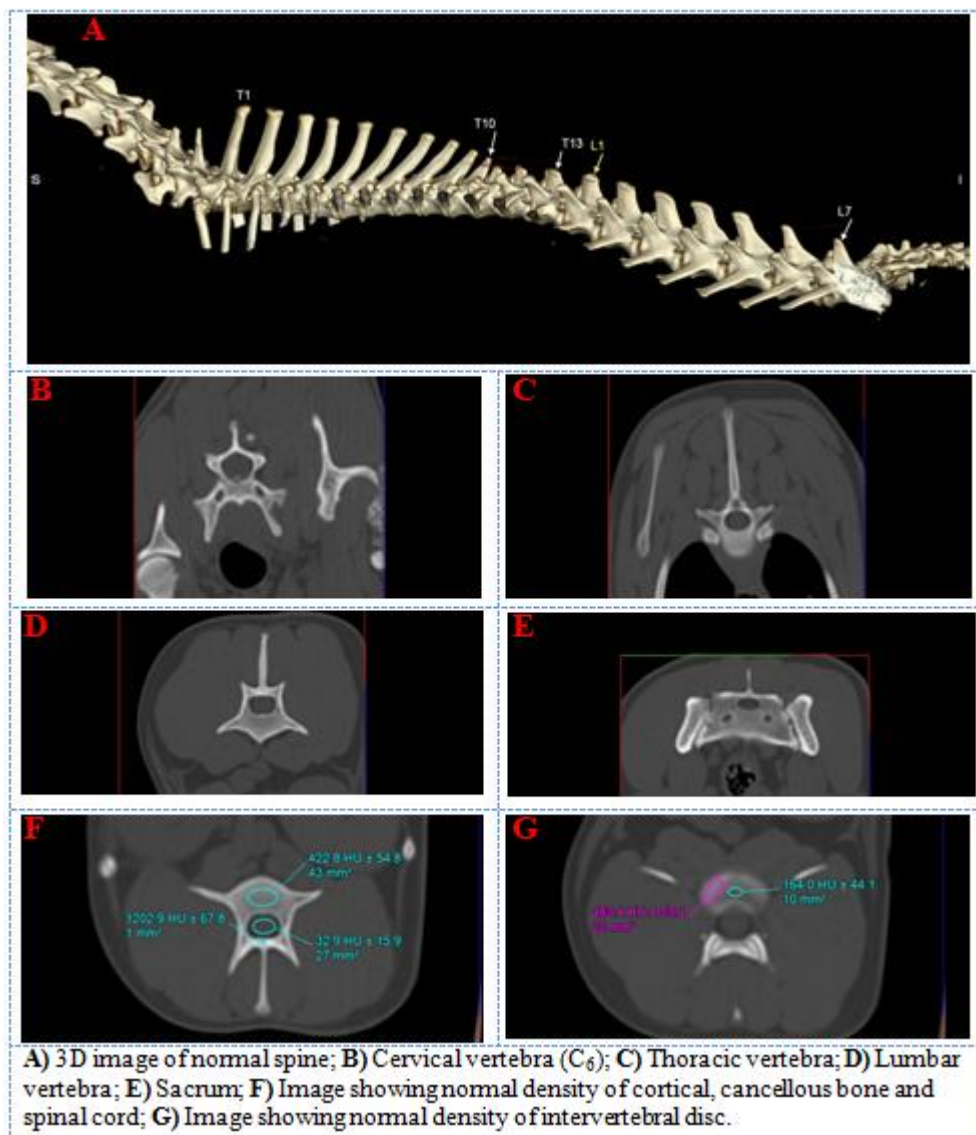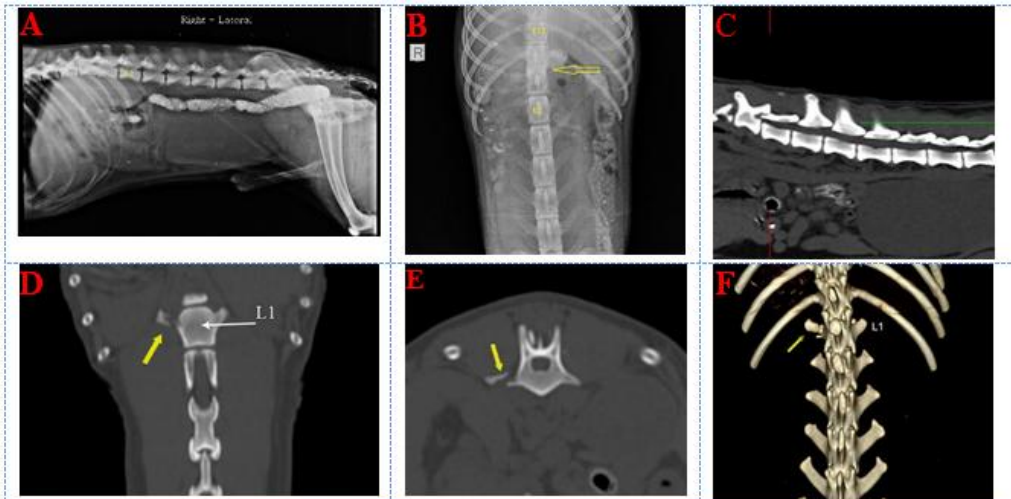
Fig. 2: Normal CT anatomy of spine

Fig. 3 A and B) Lateral and ventrodorsal radiograph showing vertebral body compression between T_{13}-L_1; **C)** Sagittal plane of thoraco-lumbar region showing disc compression between T_{13}-L_1; **D, E and F)** Coronal, Axial and 3D planes showing fracture of left transverse process.

Fig. 4 A and B) Lateral and ventrodorsal radiograph showing spondylosis from T_{13}-L_2 and between L_{6-7}; **C)** Sagittal plane of thoracolumbar region showing presence of bony proliferation at the level of T_{13} to L_2 and between L_{6-7}; **D)** Axial plane showing hypoattenuation of vertebral end plate at the level of L_6; **E)** 3D image showing spondylosis.
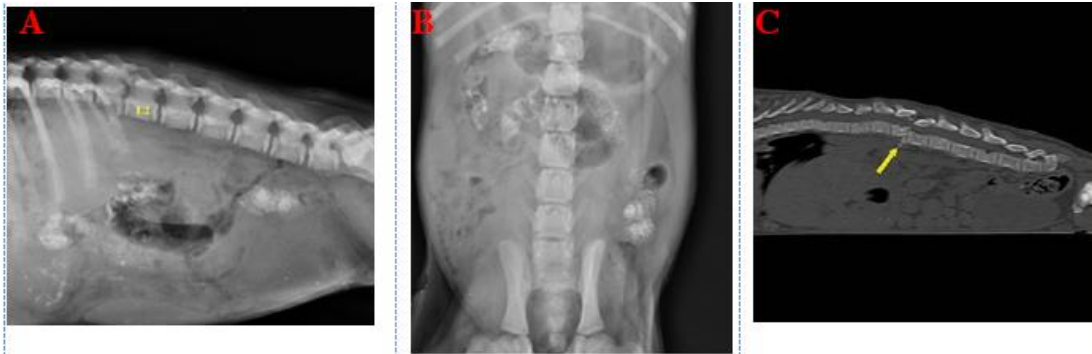
Fig. 5 A and B) Lateral and ventrodorsal radiograph showing caudal physeal fracture of L_1 vertebrae; **C)** Sagittal plane showing fracture of L_1 vertebral body with ventral luxation of caudal part; **D and E)** Axial plane showing displacement of fracture fragments in vertebral canal and fracture in all three compartments considered as unstable fracture.
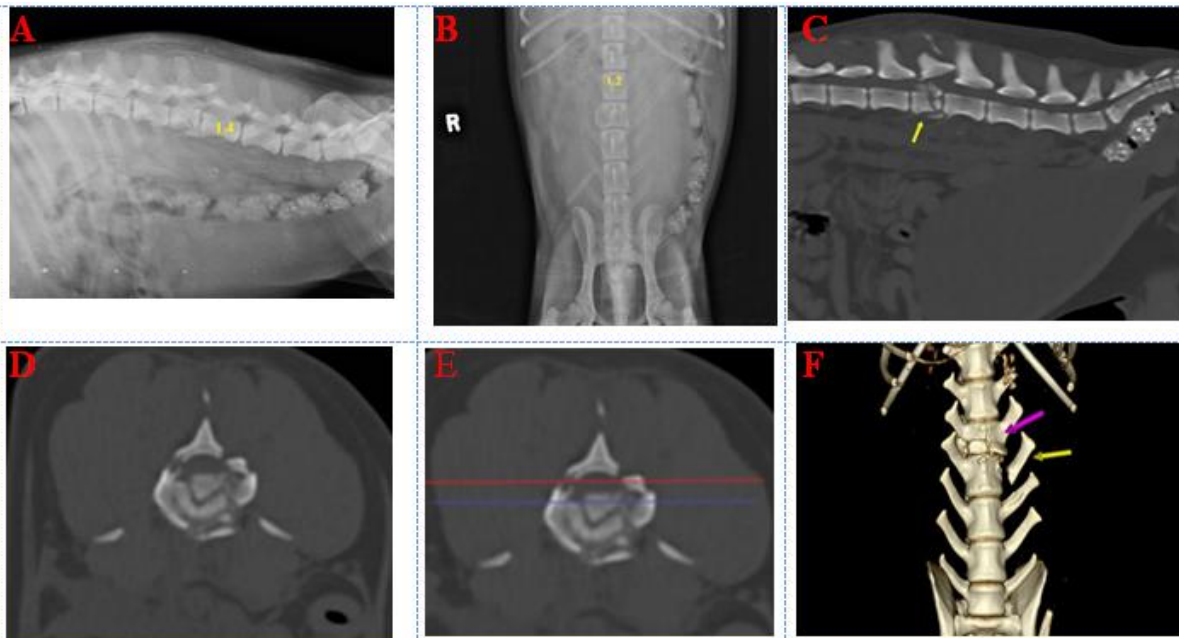

Fig. 6 A and B) Lateral and ventrodorsal radiograph showing axial compression fracture of L_3; **C)** Sagittal plane showing bursting fracture of L3; **D and E)** Axial plane showing bursting fracture at the level L_3 and fracture seen in all three compartments, considered as unstable fracture; **F)** 3D image showing axial compression fracture of L_3 and left transverse process fracture.

Fig. 7 A and B) Lateral and ventrodorsal radiograph **C, D and E)** Coronal plane, Axial plane and 3D volume rendering showing fracture of left wing of atlas along with slight luxation of the axis towards left side respectively.
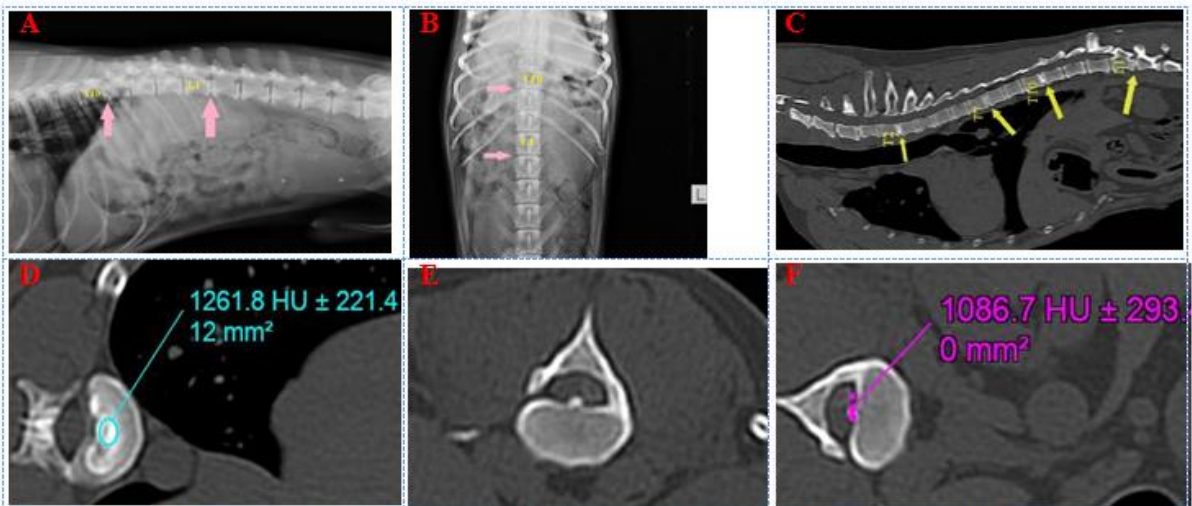

Fig. 8 A and B) Lateral and ventrodorsal radiograph showing disc mineralization between T_{10}, T_{11} and L_1, L_2 intervertebral space; **C)** Sagittal plane of thoraco-lumbar region showing disc mineralization at level of T_{2-3}, T_{7-8}, T_{10-11} and L_{1-2}; **D)** Hyperattenuating material at level of T_{10} intervertebral space; **E and F)** Transverse plane of L_1 showing round focus of hyperattenuating material in the floor of the vertebral canal, compressing the spinal cord.

REFERENCES

[1]. **Akeda, K., T. Yammada, N. Inoue, A. Nishimura and A. Sudo.** (2015). Risk factor for lumbar intervertebral disc height narrowing: a population- based longitudinal study in the elderly. *BMC Musculoskeletal Disorders*, 16: 344.

[2]. **Bagley, R.S.** (2000). Spinal fracture or luxation. *Vet. Clin. North Am. Small Anim. Pract.,* 30: 133-153.

[3]. **Bertolini, G., and M. Prokop**. (2011). Multidetector-row computed tomography: technical basics and preliminary clinical applications in small animals. *The Veterinary Journal*, 189(1): 15-26.

[4]. **Dabanoglu, I., M.E. Kara, E. Turan and M.K. Ocal.** (2004). Morphometry of the thoracic spine in German shepherd dog: a computed tomographic study. *Anat Histol Embryol*, 33(1): 53-58.

[5]. **Denny, H.R and S.J. Butterworth.** (2000). A guide to canine and feline orthopaedic surgery. Fourth edition. Blackwell sciences Ltd. Chapter-17: 175-182.

[6]. **Kinnes, J., W. Mai, Seiler., A. Zwingenberger and T. Schwarz**. (2006). Radiographic sensitivity andnegative predictive value for acute canine spinal trauma. *Vet Radiol Ultrasound*. 47: 563-570.

[7]. **Lim, C., O. K. Kweon, M. C. Choi, J. Choi and J.Yoon**. (2010). Computed tomographic characteristics of acute thoracolumbar intervertebral disc disease in dogs. *J. Vet. Sci,* 11(1): 73-79.

[8]. **Olby, N.J., K.R. Müntana, N.J. Sharp, and D.E. Thrall**. (2000). The computed tomographic appearance of acute thoracolumbar intervertebral disc herniations in dogs. *Vet Radiol Ultrasound*, 41(5): 396-402.

[9]. **Palus, V.** (2014). Neurological examination in small animals. *Macedonian Veterinary Review*, 37(1): 95-105.

[10]. **Ricciardi, M.** (2016). Usefulness of multidetector computed tomography in the evaluation of spinal neuro-musculoskeletal injuries. *Veterinary and Comparative Orthopaedics and Traumatology*, 29(01): 1-13.

[11]. **Schwarz, T., M.R. Owen, S. Long and M. Sullivan**. (2000). Vaccum disc and facet phenomenon in a dog with cauda equine syndrome. *Jam Vet Med Assoc*, 217(6):862-864.

[12]. **Taylor, S. M.** (2009). Lesion localization and the neurological examination. Small Animal Inernal Medicine. 2nd Edition. Chapter-9:983-1005.

[13]. **Tins, B**. (2010). Technical aspects of CT imaging of the spine. *Insights into imaging*, 1(5-6): 349-359.